

## Summer heat induced the decline of *Pinus taiwanensis* forests at its southern limit in humid Subtropical China

Feifei Zhou<sup>a</sup>, Zhipeng Dong<sup>a</sup>, Keyan Fang<sup>a,\*</sup>, Dongliang Cheng<sup>a,\*</sup>, Hui Tang<sup>b</sup>, Tinghai Ou<sup>c</sup>, Fen Zhang<sup>d</sup>, Deliang Chen<sup>c</sup>

<sup>a</sup> Key Laboratory of Humid Subtropical Eco-geographical Process (MOE), College of Geographical Sciences, Fujian Normal University, Fuzhou 350007, China

<sup>b</sup> Department of Geosciences, University of Oslo, P.O. Box 1022, NO-0315 Oslo, Norway

<sup>c</sup> Regional Climate Group, Department of Earth Sciences, University of Gothenburg, Box 460 S-405 30 Gothenburg, Sweden

<sup>d</sup> Key Laboratory of Western China's Environmental Systems (MOE), Lanzhou University, Lanzhou 730000, China

### ARTICLE INFO

#### Keywords:

Tree rings  
Pinus taiwanensis  
Forest decline  
Wood anatomy  
Carbon isotopes

### ABSTRACT

Warming-induced aridity has caused forest decline and mortality for many sites with water-limiting conditions. However, equatorward rear-edge *Pinus taiwanensis* trees at the Daiyun Mountains in humid subtropical China are also suffering die-backs and decline, but the roles played by heat or drought stress still remain unclear. Here, we compared the tree-ring radial width, anatomical features, stable carbon isotope ( $\delta^{13}\text{C}$ ) and intrinsic water use efficiency (iWUE) between die-back and healthy trees to elucidate potential causes driving the decline. Die-back trees showed sustained growth reductions and produced tracheids with thinner cell walls over the recent decade, indicative of reduced carbon assimilation. The climate response pattern and Vaganov-Shashkin (V-S) model indicated the critical role of summer (June–August) temperature in recent growth decline. Long-term higher wood  $\delta^{13}\text{C}$  and iWUE within die-back trees indicated that actual growth decline already started several decades earlier. This conservative growth strategy was at the cost of low efficiency of photosynthesis due to chronic stomatal closure. When the lethal heatwaves arrived, these weakened trees were not able to access sufficient carbohydrates to maintain metabolism, causing a distinct decline and mortality. We concluded that recent decline in *Pinus taiwanensis* trees was mainly caused by long-term carbon starvation.

### 1. Introduction

Forest ecosystems across many climatic zones have experienced a distinct decline in tree vigor and primary productivity for recent decades (Liu et al., 2013; Ciais et al., 2005), leading to massive shifts in vegetation biomass, composition, phenology, etc. (Allen et al., 2010; Choat et al., 2012). The warm and humid subtropical China, termed as a “green oasis” along the dry northern subtropics, is also not immune to anomalous forest decline recently (Bai et al., 2021). *Pinus taiwanensis* is an endemic tree species mainly distributed in high-elevation sites ( $\geq 800$  m), and the southernmost distribution boundary of this tree species locates in the Daiyun Mountains over the subtropical China (Chen et al., 2016). Like many forests at the low-latitude or low-altitude range margins (Peñuelas et al., 2008; Wong and Daniels, 2017; Sánchez-Salguero et al., 2017a), the rear-edge *Pinus taiwanensis* forests are also suffering from high rates of decline or die-backs in recent decade (Chen et al., 2016).

Forest declines are commonly driven by cumulative effects of multiple biotic (e.g. genetic dynamics and competition) and abiotic (e.g. disturbances and environmental stresses) processes (Lutz and Halpern, 2006; Allen et al., 2010; Cailleret et al., 2016), and complex interactions among these factors make forest declines more difficult to understand and reconstruct (Minorsky, 2003; Amoroso et al., 2015). Climate, as one of the most prominent abiotic factors, alters the structure, composition and ecological functions of forests worldwide (van Mantgem et al., 2009; Allen et al., 2010; Liang et al., 2014; Fang et al., 2015). Drought and heat stress have incited increasing rates of decline and mortality in diverse forests across the globe (Fensham et al., 2009; Adams et al., 2010; Liu et al., 2013). In addition, extensive tree die-offs also caused great alterations in hydrologic cycles, and large carbon releases from the biosphere to the atmosphere that may contribute to further warming (Breshears et al., 2007; Adams et al., 2009). Forest decline was thought to be amplified due to the increase of the frequency and intensity of hotter droughts induced by a warming climate, causing physiological

\* Corresponding authors.

E-mail addresses: [kfang@fjnu.edu.cn](mailto:kfang@fjnu.edu.cn) (K. Fang), [chengdl02@aliyun.com](mailto:chengdl02@aliyun.com) (D. Cheng).

<https://doi.org/10.1016/j.agrformet.2024.109974>

Received 19 June 2023; Received in revised form 1 March 2024; Accepted 15 March 2024

Available online 23 March 2024

0168-1923/© 2024 Elsevier B.V. All rights reserved.

stress in trees (van Mantgem et al., 2009; Allen et al., 2010; Millar and Stephenson, 2015).

Warming-induced drought stress are usually considered as the initial trigger for massive forest mortality, especially at the dry range edges (Penuelas et al., 2008; Wong and Daniels, 2016; Anderegg et al., 2019). The humid subtropical forests are also not immune to drought stress. Previous studies have indicated that summer drought strongly limited tree growth in the subtropics of China (Jing et al., 2022; Zhang et al., 2023). The critical mechanisms for tree decline under drought stress were hydraulic failure via xylem embolism or carbon starvation (Fonti et al., 2010; MacDowell et al., 2011; Adams et al. 2017), largely caused by cavitation and stomatal closure (Puchi et al., 2021). However, a growing amount of evidence have revealed that heat stress directly effect the overall performance and the survival of trees (Song et al., 2014; Breshears et al., 2021). Heat-induced tree mortality can cause abrupt decline in forest biomass stocks when temperatures reach the thermal tolerance threshold of tree's physiological function (Kunert et al., 2021). So far, the actual mechanisms causing *Pinus taiwanensis* at the Daiyun Mountains mortality are still unclear, limiting the capacity to develop suitable strategies for trees to cope with a changing climate.

The multi-proxy including radial growth, wood anatomical features and stable isotopes registered in tree rings can provide retrospective insights to disentangle the physiological mechanisms involved in forest decline (Fonti et al., 2010; Liu et al., 2013; Gessler et al., 2018). Unfavorable climate conditions (e.g. heat waves, drought, coldness) directly affect radial growth decline and a rise in synchronicity among trees (Liu et al., 2013; Camarero et al., 2015). Annual rings of declining trees also present a higher persistence and variance, and increased sensitivity to climates (Bigler and Veblen, 2009). Wood anatomical features of tree rings such as cell lumen area (CLA) and cell wall thickness (CWT) serve as a robust indicator for long-term hydraulic conductivity and carbon uptakes (Cuny et al., 2015; Castagneri et al., 2018). Carbon isotopic discrimination ( $\delta^{13}\text{C}$ ) in tree rings are useful tools to provide information on the ratio of net photosynthetic  $\text{CO}_2$  assimilation rate (A) to stomatal conductance rate ( $g_s$ ) (Farquhar et al., 1982), and quantify long-term intrinsic water use efficiency (iWUE), i.e. the cost of fixing carbon in terms of water use (Ehleringer et al., 1993). The combination of these multi-proxy approach have been adopted to assess how trees are

predisposed to climate-induced diebacks (Pellizzari et al., 2016; Gessler et al., 2018; Puchi et al., 2021).

In present work, we compare radial growth patterns and the sensitivity to climate variables between healthy and die-back trees by the dendrochronological analysis, coupled with wood anatomical traits and  $\delta^{13}\text{C}$  variations in tree rings, to gain insight into mechanisms of the decline of the *Pinus taiwanensis* at the Daiyun Mountains. Specifically, the goals of our study are (1) to reveal the disparity between die-back and healthy trees in terms of long-term growth behaviors and climate sensitivity, (2) to reveal the dominant climatic factors that drive recent tree decline, and (3) to elucidate the physiological key indicators that characterize trees with high risk for decline.

## 2. Material and methods

### 2.1. Study area and climate data

Tree-ring cores were collected from four pure mature *Pinus taiwanensis* forests at the southern Daiyun Mountains from 1550 to 1680 m a. s.l. (Fig. 1a; Table S1), mixed with various understory shrubs (e.g. *Eurya rubiginosa*, *Eurya loquaiana*, *Rhododendron latoucheae*). The main soil type underneath them is yellow soil derived from the weathered granite, with high content of water stable aggregate and organic matter (Liu et al., 2020). Many die-offs of *Pinus taiwanensis* trees have occurred in this area (Fig. 1b). The area is a transitional zone between southern and northern subtropical China, with an average annual temperature of 12.3 °C and mean annual precipitation of 1746 mm for the available period 1956–2016, according to the records from the Jiuxianshan meteorological station (118.01°E, 25.72°N, 1653 m). The warmest months are July and August, and the peak precipitation occurs from June to August when the Asian monsoon arrives at this region (Fig. 1c). In addition, the relative humidity (RH) and vapor pressure deficit (VPD) based on daily records were used to indicate regional hydroclimate changes. The VPD is the difference between the saturation vapor pressure at air temperature (T), minus the actual vapor pressure:

$$\text{VPD} = 0.611 \times 10^{(7.5 \times T / (237.3 + T))} \times (1 - \text{RH} / 100)$$

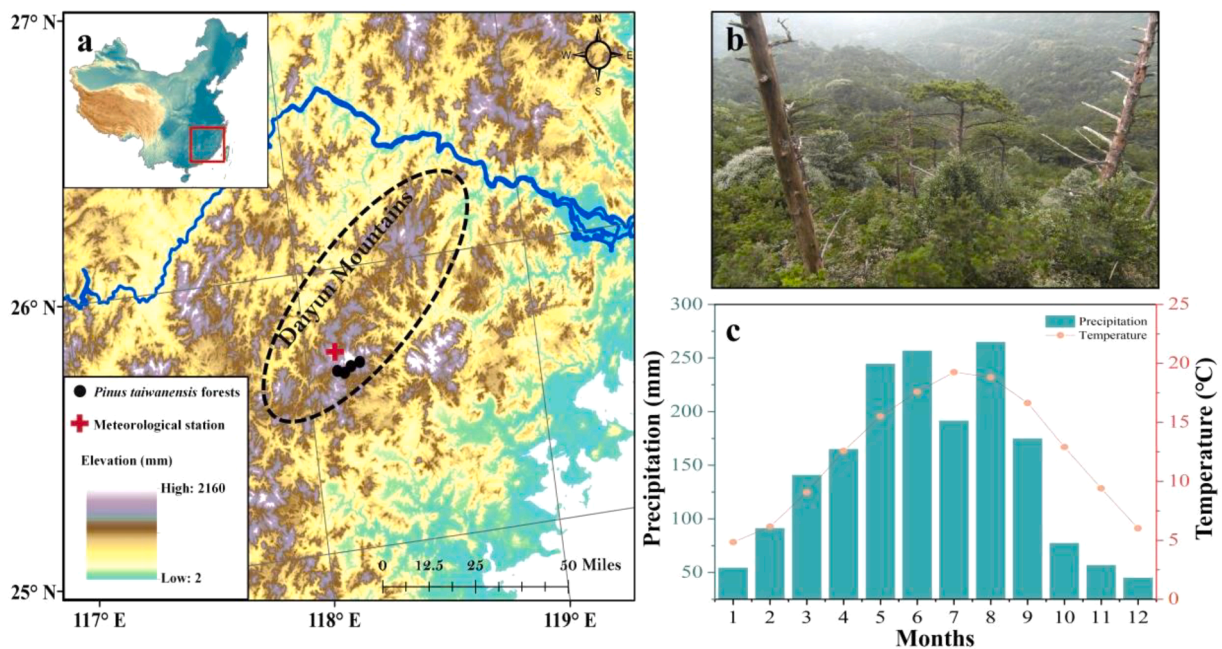


Fig. 1. a) The sampling locations of *Pinus taiwanensis* forests and Jiuxianshan meteorological station; b) Forests of *Pinus taiwanensis* in southern Daiyun Mountains; c) Monthly average temperature (dot line) and total precipitation (b bar) from the meteorological station during the 1956–2015 period.

## 2.2. Sample collection and tree-ring width analysis

We totally sampled 346 increment cores from a total of 173 living adult trees at breast height at the four sites. Given that these sites were very close and sampled trees grew in a similar habitat, we grouped all these tree-ring samples for crossdating. Firstly, all these samples were classified into two groups, 71 from decline trees and 102 from healthy trees. For determination of the health status, healthy trees showed no sign of crown die-back, whereas die-back trees showed defoliation in  $\sim 30\%$  of the crown estimated by four observers for the reduction of subjective errors (Petrucco et al., 2017). After air drying and sanding, tree-ring radial width (TRW) of the cores were measured and crossdated at  $\pm 0.001$  mm precision with a LINTAB system. The COFECHA program was further employed for the quality control of crossdating (Homes, 1983). Many annual rings of die-back trees were devitalized during recent decades and thus were excluded for the development of the chronology. Then the growth trend in the raw measurements was removed by fitting negative exponential curves or linear regression curves of any slope. The trees were excluded for the chronology development in a few cases when anomalous growth trends occurred. The tree-ring indices were calculated as ratios between raw measurements and the fitted growth values, and then merged to develop a biweight robust mean chronology of die-back and healthy groups, respectively (Cook, 1985). We then averaged all of the standardized tree-ring series to obtain the final TRW index for each group (Fig. 2a). The subsample signal strength (SSS) with a threshold value of 0.85 was employed to evaluate the most reliable period of the chronology (Wigley et al., 1984). The standard tree-ring width chronologies of die-back and healthy groups were established, and the reliable intervals started from 1911 to 1910, respectively (Figs. 2b, 2c).

## 2.3. The Vaganov-Shashkin model

The process-based Vaganov-Shashkin (V-S) model permits us to investigate features of TRW variations under specific environmental conditions linking temperature, soil moisture and day length (Vaganov et al., 2006). In this model, the simulated growth rate due to sunlight is defined by the harmonic function depending on geographic location (Gates, 1980), and the partial influence of temperature and soil moisture on tree-ring formation are both defined by piece-wise linear functions (Vaganov et al., 2006; Evans et al., 2006). The modeled tree growth rate is largely determined by the primary limiting factor between temperature and soil moisture. The V-S model is multi-parametric, and the descriptions suggested by previous literature (Shi et al., 2008; Gou et al., 2013) and physiological observations of *Pinus taiwanensis* (Zhu, 2013) were followed to determine biologically reasonable parameters. However, physiological process and water-use efficiency of conifers were very different across regions (Touchan et al., 2011; Timofeeva et al., 2017; Colangelo et al., 2017; Pellizzari et al., 2016; Puchi et al., 2021), and we adjusted a few parameters to guarantee a good agreement of hypothetical and observed tree-ring chronologies of decline trees through repeated trial. A split-sample procedure that divided the full period (1956–2016) into two subsets was also used to verify model stability. The model was firstly applied to simulate the chronology for 1956–1986 to estimate the optimal parameters (Table S2), and we then tested the performance of the model with the rest data (1987–2016).

## 2.4. Quantification of wood anatomical features

We investigated anatomical features of annual rings from five mature die-back and healthy trees with similar age ( $\sim 90$  yr) and homogeneous growth patterns, respectively. The cross-sections ( $15\ \mu\text{m}$ ) of annual rings of these selected cores were cut by using a Reichert sliding microtome for 1920–2016. Microsections were then stained with a solution of 1%

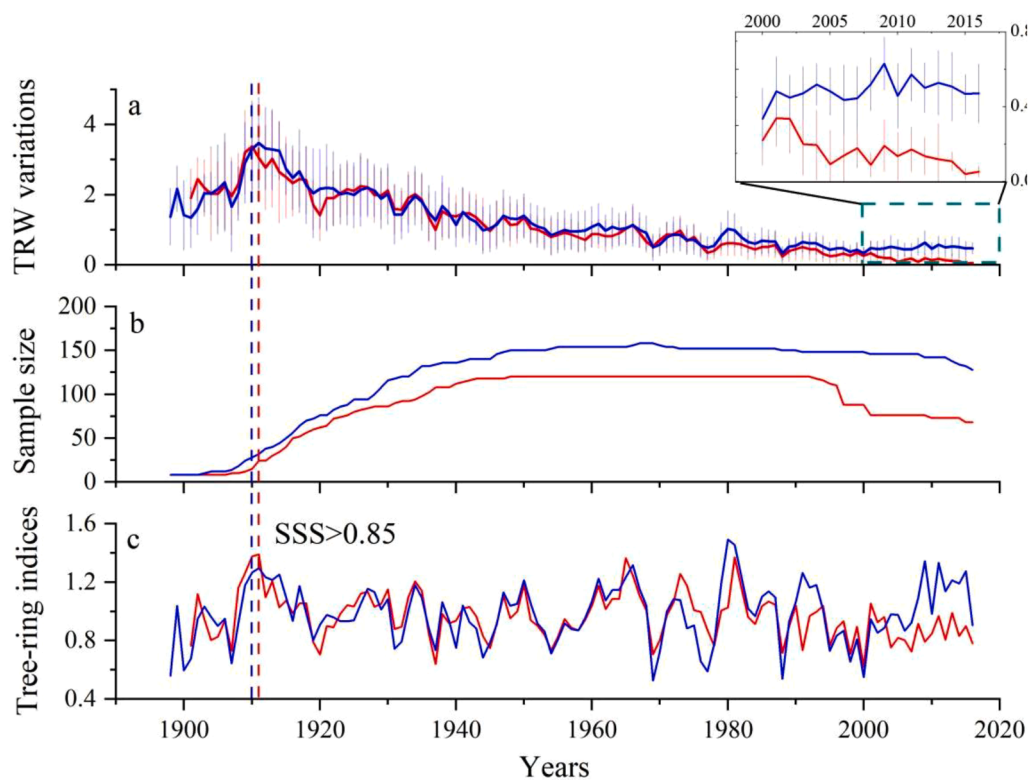


**Fig. 2.** a) Mean tree-ring width variations (TRW) with standard deviation (bar), b) sample size and c) standard width chronologies of die-back (red line) and healthy (blue line) *Pinus taiwanensis* trees in Daiyun Mountains. The vertical dash lines denote the calendar years with  $\text{SSS} > 0.85$ . The comparison between the TRW of die-back and healthy trees for 2000–2016 is highlighted in the inserted box.

alcohol solvable safranin, dehydrated with alcohol (35, 50, 75, 95 and 100%) and immersed in xylol (Schweingruber, 1990). The stained microsections were mounted on glass slides, embedded with a hardening epoxy and dried. Then they were observed and photographed with the WINCELL imaging system. The 50th percentile of the conduit lumen area (CLA<sub>50</sub>) and theoretical hydraulic conductivity (K<sub>t</sub>) of earlywood and latewood based on the Hage-Poiseuille's law were calculated to investigate water transport efficiency (Tyree and Zimmermann, 2002; Fonti et al., 2010). The CWT variations of earlywood and latewood were used as an indicator of carbon allocations for annual rings (Petrucco et al., 2017).

## 2.5. Analysis of carbon isotopes and intrinsic water use efficiency

We selected ten cores from six trees in healthy and decline groups with homogeneous growth patterns for isotopic analysis, respectively. Annual rings from different trees formed in the same year were cut off, pooled and stored in microcentrifuge tubes (Leavitt, 2008). The "pooling" method was reliable in the subtropical China based on the high coherency of tree-ring isotopic data of cores from different trees (Li et al., 2016; Guo et al., 2017). Then  $\alpha$ -cellulose of the annual tree rings was purified following a modified method of Green (1963) and Loader et al. (1997). To homogenize the cellulose, an ultrasonic water bath (JY92-2D, Scientz Industry, Ningbo, China) was used to break the cellulose fibers (Leavitt and Long, 1984; Laumer et al., 20,010). The carbon isotope ratios were measured using the Flash Elemental Analyzer (Flash 2000) coupled with a Thermo Scientific MAT 253 (Thermo Electron Corporation, Bremen, Germany). Each sample was repeatedly measured four times to determine the stability and the mean values. Results are expressed as  $\delta^{13}\text{C}$ , in per mille (‰) relative to the Vienna Pee Dee Belemnite (VPDB) standard (Coplen, 1995):

$$\delta^{13}\text{C} = \left[ \left( \frac{R_{\text{sample}}}{R_{\text{standard}}} - 1 \right) \right] * 1000$$

where  $R_{\text{sample}}$  and  $R_{\text{standard}}$  indicate the  $^{13}\text{C}/^{12}\text{C}$  ratios of  $\alpha$ -cellulose sample and VPDB standard, respectively. The accuracy of the isotopic measurements were 0.07‰.

The isotopic discrimination ( $\Delta$ ) between the carbon of atmospheric CO<sub>2</sub> and plants was defined as (Farquhar et al., 1982):

$$\Delta = (\delta^{13}\text{C}_a - \delta^{13}\text{C}_p) / (1 + \delta^{13}\text{C}_p / 1000) = a + (b - a)(c_i / c_a)$$

where  $\delta^{13}\text{C}_a$  and  $\delta^{13}\text{C}_p$  are the isotope ratios ( $^{13}\text{C}/^{12}\text{C}$ ) of carbon in atmospheric CO<sub>2</sub> and plant cellulose, respectively;  $a$  ( $\approx 4.4\%$ ) represents the fractionation during CO<sub>2</sub> diffusion through the stomata, and  $b$  ( $\approx 27\%$ ) is the fractionation due to the carboxylation;  $c_i$  and  $c_a$  symbolize the intercellular and ambient CO<sub>2</sub> concentrations. The values of  $\delta^{13}\text{C}_a$  are obtained from ice core and atmospheric data proposed by MaCarroll and Loader (2004). Finally, the iWUE can be calculated as follows (Ehleringer et al., 1993):

$$\text{iWUE} = A/g_s = (c_a - c_i) / 1.6 = c_a(1 - c_i / c_a) / 1.6$$

## 2.6. Statistical analysis

Pearson's correlations between the tree-ring width chronology and monthly climate records over 1956–2016 are calculated to reveal the dominant factors that modulated radial growth of *Pinus taiwanensis* trees, as well as check the coherency between observed and simulated tree-ring records. To test the temporal stability of the coupling relationships between tree growth and carbon isotopes, 31-a moving correlations between TRW and  $\Delta^{13}\text{C}$  were calculated for 1920–2016 period. The statistical significance of the difference of anatomical features between die-back and healthy trees was checked by using the Mann-Whitney U (MWU) test (Grissom and Kim, 2012). A linear regression model was used to detect long-term trends of climate variables. The sequential Mann-Kendall (M-K) test proposed by Sneyers

(1991) was used to indicate the approximate year of the beginning of a significant trend in climate change. This test sets up two series, a forward one (UF<sub>k</sub>) and a backward one (UB<sub>k</sub>). If they cross each other and diverge beyond the specific threshold value ( $\pm 1.96$ ), then there is a statistically significant ( $p < 0.05$ ) trend. The point where UF<sub>k</sub> and UB<sub>k</sub> cross each other indicates the approximate year at which the trend begins (Mosmann et al., 2004). The first to 20th-order auto-correlations for the  $\Delta^{13}\text{C}$  chronologies of die-back and healthy trees were used to investigate the degree of dependence on carbon reserves.

## 3. Results

### 3.1. Growth patterns and responses to climate

Die-back *Pinus taiwanensis* trees showed slightly different TRW growth patterns with healthy ones, with a distinct ( $p < 0.01$ ) differentiation between them starting to emerge since the 21st century (Fig. 2a). The relationships between the two chronologies and monthly climate records were assessed for their common period of 1956–2016 (Fig. 3). No significant correlations were found between the die-back chronology and monthly precipitation, instead we found a positive and significant ( $p < 0.05$ ) correlation with summer (June–August) temperature (Figs. 3a, 3b). In contrast, the healthy chronology showed no significant correlations with temperature (Fig. 3b). However, we found significant negative correlations with previous December and current January precipitation (Fig. 3b). In addition, the die-back and healthy chronologies both significantly ( $p < 0.05$ ) and negatively (positively) correlated with RH (VPD) changes in January during the pre-growing season (Figs. 3c, 3d).

### 3.2. Regional climate variability

We investigated the long-term trends of seasonal climate variables that were sensitive to tree growth of *Pinus taiwanensis* (Figs. S1, S2). Mean temperature and RH records in the study area for the summer season have increased significantly during 1956–2016 (Temperature:  $R^2=0.22$ ,  $p < 0.01$ ; RH:  $R^2=0.09$ ,  $p < 0.05$ ) (Figs. S2a, S2c). Consistent with the RH increase, summer VPD maintained a significant downward tendency for recent decades ( $R^2=0.09$ ,  $p < 0.05$ ). Though less pronounced, regional summer precipitation showed a positive trend ( $R^2=0.02$ ,  $p < 0.1$ ). Therefore, summer hydroclimate at the Daiyun Mountains exhibited a notable wetting tendency over the past decades. In contrast, the hydroclimate during the pre-growing season (December–January) had no significant trends (Fig. S2). Interestingly, we found that the significant trend in summer temperature started since 2003 until 2016, revealed by the M-K test (Fig. 4). This increase of summer temperature was in concomitant with the drastic reduction of TRW in die-back trees.

### 3.3. Simulated tree growth with the V-S model

Based on the estimated optimal parameters in the V-S model (Table S2), we found a significant positive correlation ( $r = 0.72$ ,  $p < 0.001$ ) between the simulated and observed tree-ring chronologies of die-back trees for the calibration period 1956–1986 (Fig. 5a). Then we used these parameters to model tree growth for 1987–2016, an independent period not used in the calibration. A strong correlation ( $r = 0.59$ ,  $p < 0.001$ ) between them highlighted that the process-based V-S model has excellent skill in simulating and interpreting tree-ring formation as well as reproducing growth response patterns to climate for die-back *Pinus taiwanensis* trees at the Daiyun Mountains. The model-calculated partial growth rates due to temperature were lower than those due to soil moisture throughout the entire growing season (Fig. S3a). We further examined the difference in intra-annual growth before (1956–2003) and during (2003–2016) the distinct decline. The notable disparity of the modeled growth rates between the two intervals

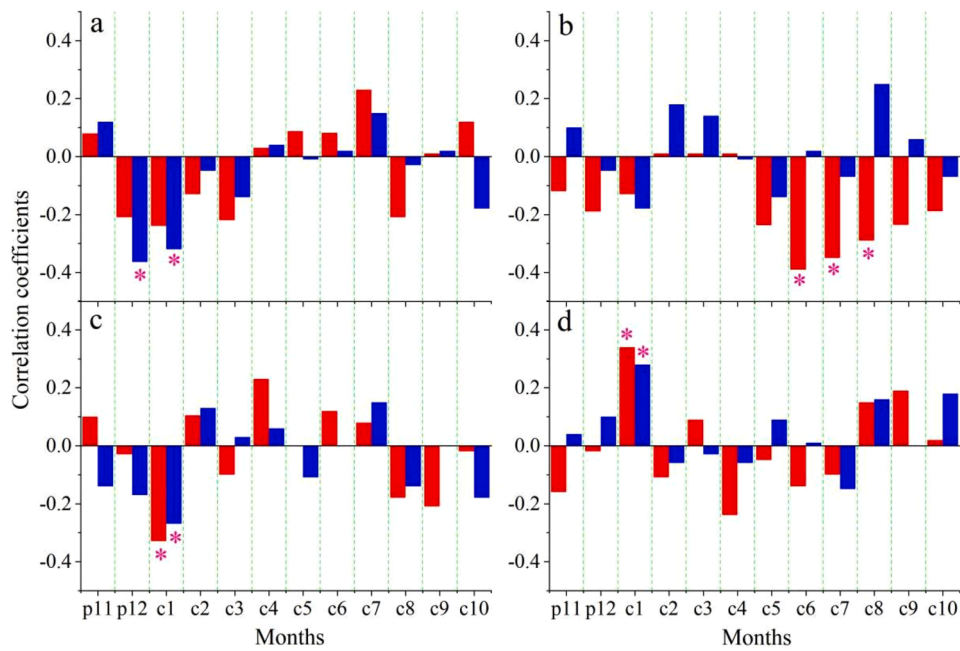


Fig. 3. Climate correlations between die-back (red bar) and healthy (blue bar) tree-ring chronologies with monthly (a) total precipitation, (b) mean temperature, (c) relative humidity, and (d) VPD recorded by Jiuxianshan meteorological station from previous November to current November over the common period of 1956–2016. Correlations significant at the 95% level have been indicated by the asterisks.

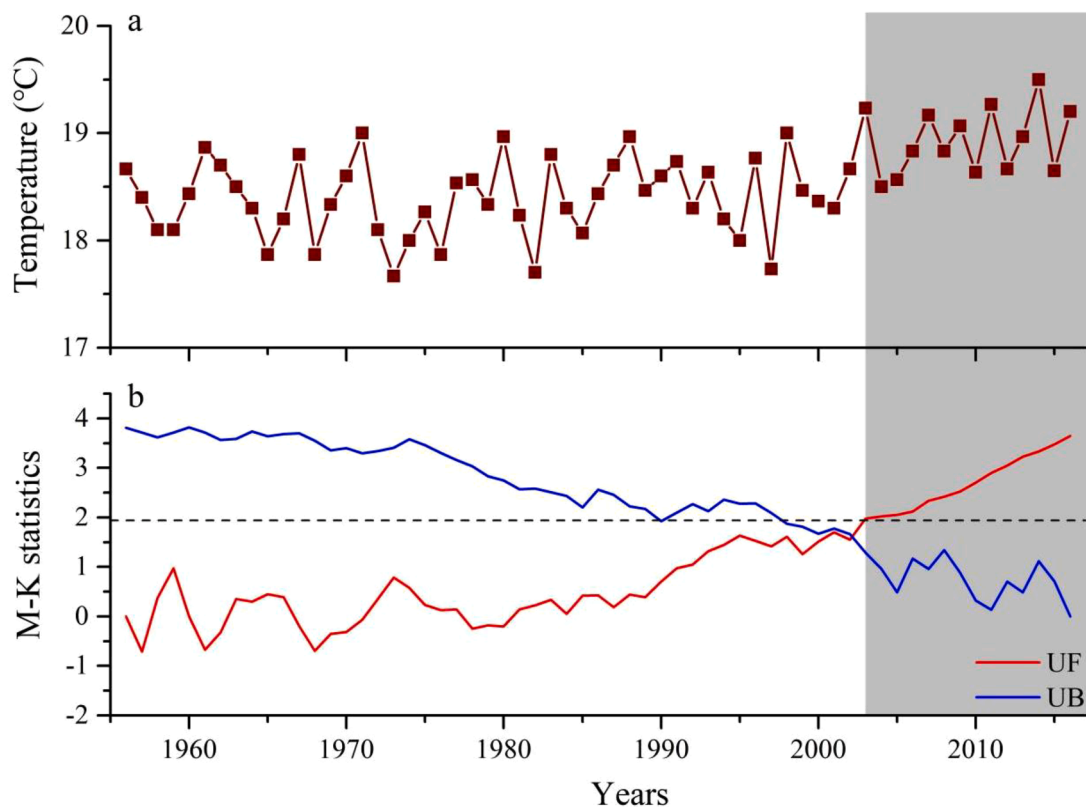
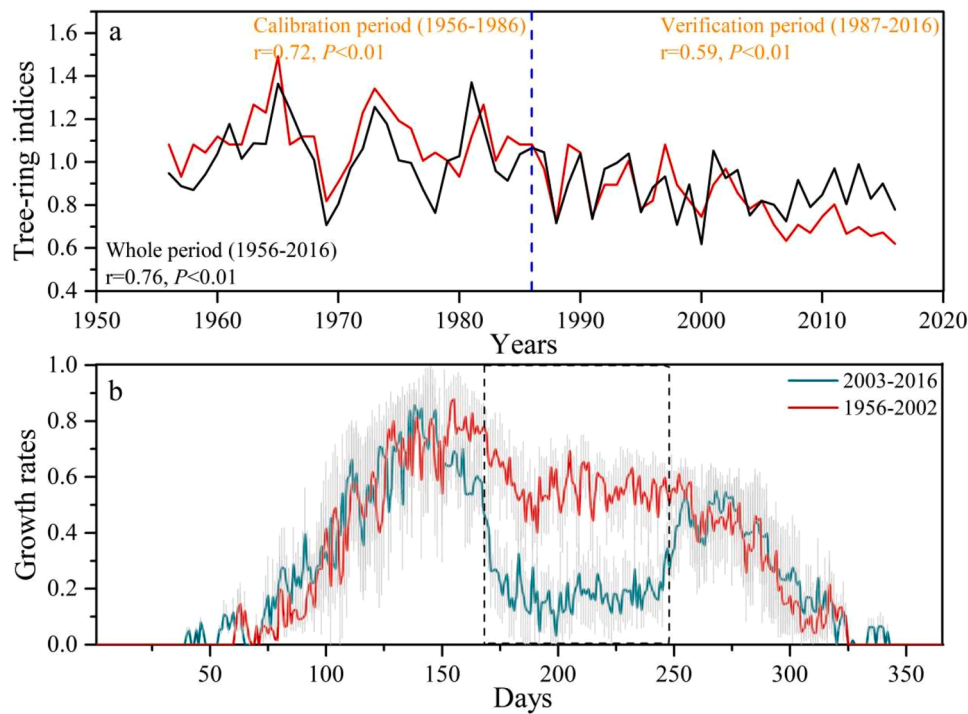


Fig. 4. (a) Summer temperature between the period from 1956 to 2016 and (b) the statistics tested by the M-K method.

mainly occurred in summer (Fig. 5b). The growth decline in summer caused the intra-annual growth pattern progressively changing from unimodal to bimodal in recent decades (Fig. 5b).

### 3.4. Carbon isotopes and *iWUE*

The tree-ring  $\delta^{13}\text{C}$  ( $\Delta^{13}\text{C}$ ) values of healthy trees were notably ( $p < 0.05$ , the MWU test) higher (lower) than those of die-back ones (Figs. 6a, 6b). The  $\Delta^{13}\text{C}$  series of the two groups showed very different climate



**Fig. 5.** a) Comparison between the observed (black) and simulated (red) tree-ring width chronologies for calibration period (1956–1986) and verification period (1987–2016); b) Modeled mean growth rates during the 2003–2016 and 1956–2002 periods, respectively. The shaded areas symbolize the mean and  $\pm$  SE.

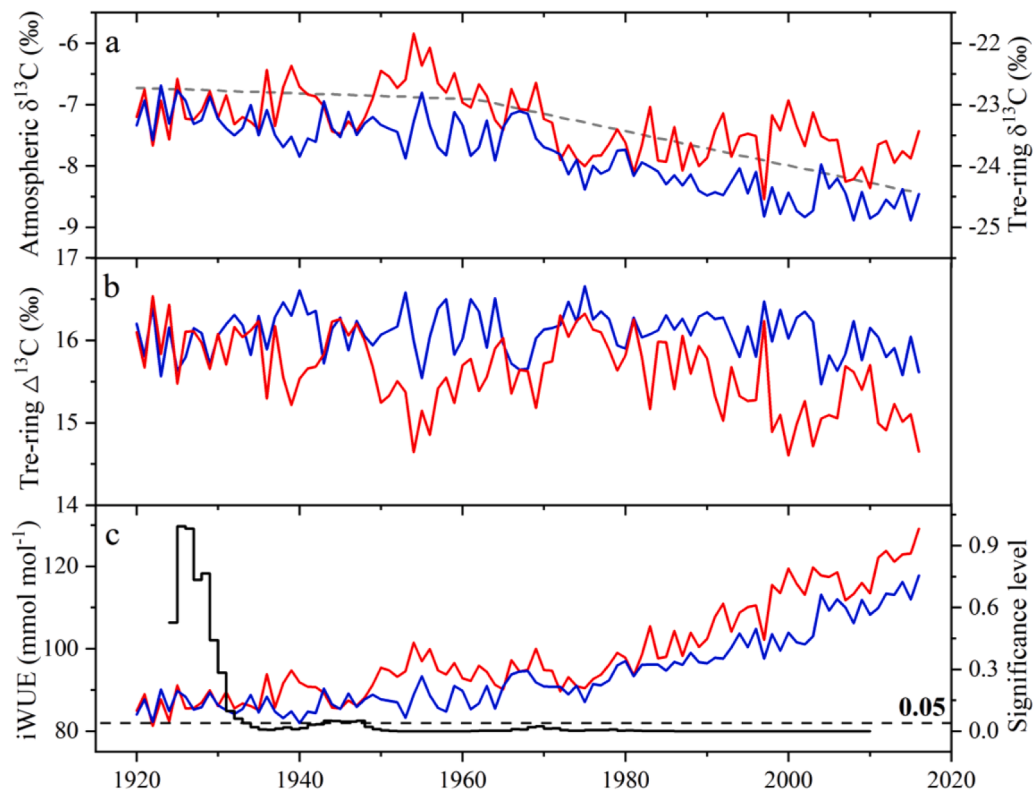


**Fig. 6.** a) Tree-ring  $\delta^{13}\text{C}$  chronologies for die-back (red line) and healthy (blue line) *Pinus taiwanensis* trees and atmospheric carbon isotope ratio (dash line) for the 1920–2016 period; b) Corrected tree-ring  $\delta^{13}\text{C}$  ( $\Delta^{13}\text{C}$ ) chronologies based on the method of [McCarroll and Loader \(2004\)](#); (c) The iWUE chronologies and the significance level of the difference between them tested by the moving MWU test with a 11-a window. The dash line indicates the 0.05 significance level.

response patterns. For the  $\Delta^{13}\text{C}$  of die-back trees, significant ( $p < 0.05$ ) negative correlations with temperature were found in late spring and summer (Fig. S4). The  $\Delta^{13}\text{C}$  of healthy trees showed significant ( $p < 0.05$ ) correlations with precipitation, RH and VPD in October (Fig. S4). A sustained increase in iWUE for the past decades derived from tree-ring  $\delta^{13}\text{C}$  was observed for both groups (Fig. 6c). However, in agreement with  $\delta^{13}\text{C}$  values, die-back trees presented higher iWUE than healthy ones, especially since the 1930s (Fig. 6c). For die-back trees, TRW growth and  $\Delta^{13}\text{C}$  values were significantly positively correlated ( $R^2=0.21, p < 0.01$ ), but for healthy trees there was no relationship at all (Fig. 7a). The connections between TRW and  $\Delta^{13}\text{C}$  in die-back trees became strengthened since the 1950s (Fig. 7b). In addition, we found that the first-order temporal autocorrelations were positive and significant for die-back trees in  $\Delta^{13}\text{C}$ , but insignificant for healthy trees (Fig. S5).

### 3.5. Anatomical features

Wood anatomy traits including the  $\text{CLA}_{50}$ ,  $K_h$ , CWT of earlywood and latewood were investigated in die-back and healthy trees for the period of 1956–2016. Both die-back and healthy trees did not produce notably distinct tracheids, in comparison with those developed before the decline period (1956–2002). In addition, the  $\text{CLA}_{50}$  and  $K_h$  variations of earlywood in both groups did not differ significantly during the growth decline period (2003–2016). While, consistent with the recent decline, thinner cell walls for the whole rings were produced in die-back trees, according to significant difference in the CWT variations of earlywood and latewood between die-back and healthy groups ( $p < 0.01$ ) (Table 1). We correlated the CWT parameters with monthly climate variables, and found that temperature in June was significantly and negatively ( $p < 0.05$ ) associated with the CWT of die-back trees (Figure S6).

**Table 1**

Statistics of the anatomical features of die-back and healthy *Pinus taiwanensis* trees at the Daiyun Mountains.

	Over the decline period (2003~2016)		Before the decline period (1956~2002)	
	Die-back	Healthy	Die-back	Healthy
$\text{CLA}_{50}$ of earlywood ( $\mu\text{m}^2$ )	643.0 ± 18.7	644.7 ± 20.5	631.3 ± 17.5	633.4 ± 16.8
$\text{CLA}_{50}$ of latewood ( $\mu\text{m}^2$ )	151.2 ± 8.5	155.7 ± 9.9	153.1 ± 9.5	156.8 ± 6.3
$K_h$ ( $\text{kg m Mpa}^{-1} \text{ s}^{-1}$ ) $10^{-15}$	2.03 ± 0.06	2.37 ± 0.09	2.28 ± 0.08	2.30 ± 0.11
CWT of earlywood ( $\mu\text{m}$ )	3.04 ± 0.04 <sup>a</sup>	3.89 ± 0.05 <sup>b</sup>	3.84 ± 0.05	3.92 ± 0.09
CWT of latewood ( $\mu\text{m}$ )	5.89 ± 0.06 <sup>a</sup>	6.55 ± 0.09 <sup>b</sup>	6.27 ± 0.06	6.41 ± 0.07

Data are presented as means ± SD in different years or periods. Different letters indicate significant ( $p < 0.01$ ) difference based on the Mann-Whitney U test. Abbreviations of variables are:  $\text{CLA}_{50}$ , the 50th percentile of conduit lumen area;  $K_h$ , the theoretical hydraulic conductivity; CWT, the cell wall thickness.

## 4. Discussion

### 4.1. Heat stress causes the decline of *Pinus taiwanensis* at its southernmost limits

Pluvial conditions in winter of the pre-growing season impacted radial growth of *Pinus taiwanensis* at the Daiyun Mountains. An excess of rainfall usually cohered with fall of temperature and lower sunshine hours, causing a decline of absorption activities of root systems and photosynthesis performance (Lovejoy and Schertzer, 2006; Zhou et al., 2019). The reductions of carbon reserves before the growing season may limit cambial activity at the early growth stage and the formation of narrow rings. Such climate-growth response patterns were also reported for the forests growing at the extremely humid habitats (Buckley et al., 2007; Soliz-Gamboa et al., 2011; Zhou et al., 2019). However, the hydroclimate in winter of the pre-growing season showed no significant

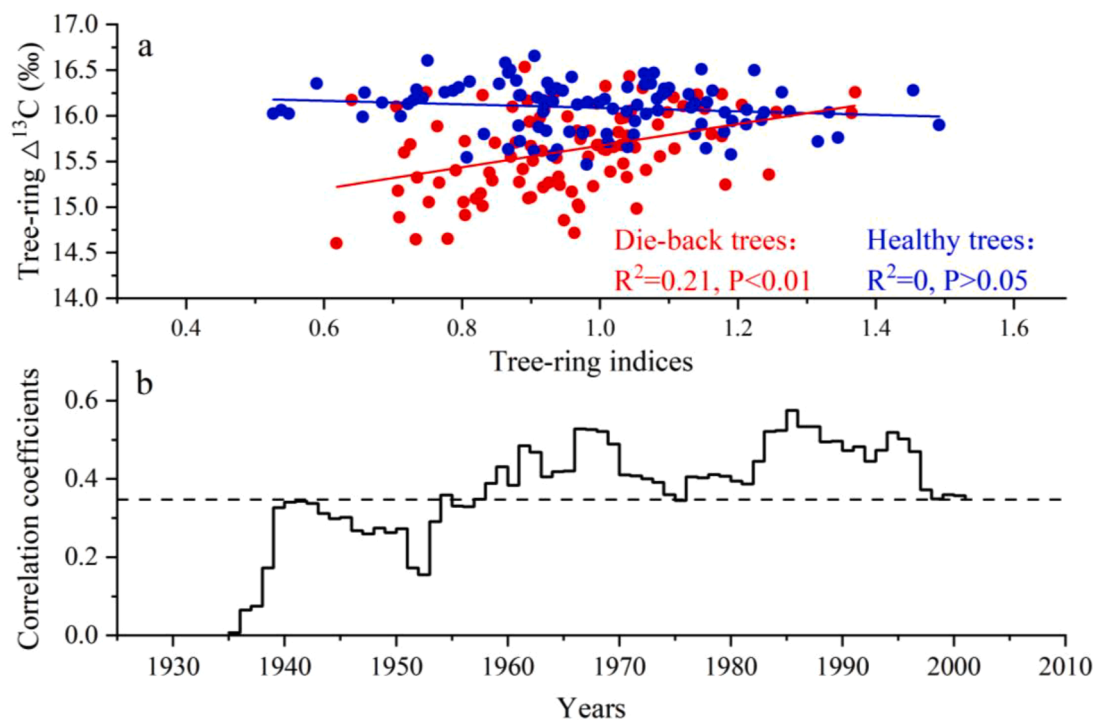


**Fig. 7.** (a) Relationships between tree-ring growth and  $\Delta^{13}\text{C}$  variations for die-back (red) and healthy (blue) *Pinus taiwanensis* trees for 1920–2016; (b) The 31-a sliding correlations between TRW and  $\Delta^{13}\text{C}$  of die-back trees. The dash line represents the significance level of 0.05.

trends over the past decades, and cannot be the determining factor for tree mortality. Unlike healthy trees, the recent growth decline of die-back trees was consistent with a notable increase in summer temperature. In this case, an increase in drought stress induced by a warming climate was typically assumed to be the determining factor for forest decline (Chen et al., 2016). Nevertheless, no significant relationships were observed between TRW variations and summer hydroclimate records. We thus hypothesized that summer heat stress directly cause the recent decline in *Pinus taiwanensis* trees instead of warming-induced drought stress.

This hypothesis was verified by the outputs of the V-S model for intra-annual growth process of die-back trees. The V-S model indicated that the minimum temperature for cambial activity of *Pinus taiwanensis* in the study area was 16 °C, much higher than trees growing in polar and alpine areas (Evans et al., 2006; He et al., 2016; Sánchez-Salguero et al., 2017b). Recent micro-observations have revealed that cambial activity of *Pinus massoniana* at high-elevations sites (~1000 m) in the subtropics of China did not start until the temperature reached ~16.5 °C (Zheng, 2023). This finding was consistent with the output of our V-S model. The distinct disparity of the growth rates between years before and after the decline mainly occurred in summer, in good agreement with independent statistically-based conclusions above. These results were very different from the stimulation cases in the cold or dry regions, where warming-induced reductions in soil moisture played a key role in tree growth (Evans et al., 2006; He et al., 2016). Elevated summer temperature caused a growth bimodality of *Pinus taiwanensis* trees at the Daiyun Mountains in recent decade. This progressive shift of intra-annual growth pattern indicated that heat stress may approach or even reach the thermal tolerance threshold, causing abrupt reductions in the photosynthetic efficiency and health deterioration in trees (Song et al., 2014; Kunert et al., 2021; Pacheco et al., 2018). Recent mass die-offs of *Pinus taiwanensis* suggested that many individuals failed to acclimate to heat stress.

#### 4.2. Carbon starvation under heat stress

Long-term wood anatomical traits were useful for unraveling ecophysiological changes associated with climate during carbon fixation (Fonti et al., 2010). The  $CLA_{50}$  and  $K_h$  variations of annual rings were usually responsive to changes in water transport systems for trees impacted by drought or heat waves (Heres et al., 2014; Fonti and Babushkina, 2016). Nevertheless, in our study, both of the two variables of *Pinus taiwanensis* trees did not show distinct variations in concomitant with summer heat stress and growth reductions, indicative of a weak effect of water availability on wood formation.

Heat stress can also cause morphological and physiological changes in tree rings of defoliated trees, which could adversely affect the resistance to disturbances (Ashraf and Harris, 2013; Song et al., 2014). Recent inferior growth performance in die-back trees cohered with the formation of thinner CWT in annual rings, suggestive of limited carbon assimilation due to reduced photosynthetic rates (Cuny et al., 2014; McDowell et al., 2008; Pellizzari et al., 2016; Petrucco et al., 2017; Puchi et al., 2021). To our knowledge, hydraulic safety of die-back trees was largely dependent on the mechanical strength of conduits, with thinner cell walls corresponding to lower resistance to embolism (Fonti et al., 2010; Petrucco et al., 2017). We interpreted this CWT depletion as increased carbon starvation in die-back trees, posing a serious threat to tracheid implosion and thus causing the decline and mortality. In addition, this behavior put trees at a higher risk of pathogens and insect attacks (MacDowell et al., 2011; Bai et al., 2021)

#### 4.3. Early warning signals of tree decline

Only a slight disparity was observed for TRW and wood anatomy of die-back and healthy trees before the distinct decline, but the actual decline in die-back trees had started since the 1930s, according to higher

long-term  $\delta^{13}C$  and iWUE variations. Given a distinct depletion of photosynthetic rates in die-back trees under heat stress, we attributed this rise in iWUE into decreased stomatal conductance. The critical mechanism for tree performance and survival under unfavorable conditions was dependent on the capacity to produce sufficient fresh carbohydrates to support metabolism and enhance resistance to disturbances (McDowell et al., 2011). Carbon starvation intensified when stoma closed, hindering the formation and transport of photosynthetic carbohydrates in phloem (McDowell et al. 2008; Timofeeva et al., 2017). In addition, heat stress threatened leaf surface safety temperature and impaired stomatal regulation of die-back trees, causing an increase in light respiration and a decrease in carbon reserves (McDowell et al., 2011; Marchin et al., 2021).

At the early phase, radial growth seemed to be affected slightly possibly due to stored carbohydrates, but the development of fine roots and needle mass might be hindered due to limited carbon allocation (Dobbertin et al., 2010). This behavior as a consequence weakened tree vigor by impairing nutrient uptake and photosynthetic carbon assimilation. The growth and leaf gas-exchange became strengthened since the 1950s, and both of them were strongly coupled with summer temperature. These findings indicated that reduced carbohydrates induced by heat stress have directly impacted the xylem cell production in the stem.

Instead, healthy trees had a higher stomatal conductance, which cooled leaves to avoid the damaging temperature and was in favor of carbon uptake (Marchin et al., 2021). The different strategies implied different levels of resistance to embolism for different individuals (Petrucco et al., 2017). Conspicuous auto-correlations in  $\delta^{13}C$  variations suggested that the growth and physiology of die-back trees were strongly dependent on carbon reserves of the previous growing season. Low  $\delta^{13}C$  variance could also be a good indicator of early-warnings of impending mortality (Camarero et al., 2015). Tree decline and mortality occurred when the stored and freshly synthesized carbohydrates failed to support tree growth and physiology. Overall, the distinct decline over the past decade could be a combined result of intensified heat stress and previous long-term weakening process due to reduced carbon uptake.

## 5. Conclusions

The notable increase of summer warming observed in the recent decade was the most likely factor for the widespread decline and mortality in *Pinus taiwanensis* at the Daiyun Mountains of humid subtropical China. Heat stress might cause the closure of the stomata, leading to a reduction in photosynthetic activity and carbon assimilation in die-back trees. In addition, long-term high wood  $\delta^{13}C$  values in die-back trees suggested that growth decline actually started several decades earlier. The provident growth strategy of die-back trees could not satisfy the carbon demand of the root and needle mass development and thus reduced the carbon uptake in the long term. The arrival of sustained heatwaves in summer aggravated the forest decline due to lower availability of carbohydrates. An expected increase in summer temperature over southeastern China will put *Pinus taiwanensis* forests in a higher risk of decline in the future.

#### CRedit authorship contribution statement

**Feifei Zhou:** Writing – original draft, Conceptualization. **Zhipeng Dong:** Investigation, Data curation. **Keyan Fang:** Writing – review & editing, Supervision, Conceptualization. **Dongliang Cheng:** Validation, Supervision. **Hui Tang:** Writing – review & editing, Methodology. **Tinghai Ou:** Writing – review & editing, Software. **Fen Zhang:** Methodology, Investigation, Data curation. **Deliang Chen:** Writing – review & editing, Supervision, Funding acquisition.

#### Declaration of competing interest

The authors declare that they have no known competing financial

interests or personal relationships that could have appeared to influence the work reported in this paper.

## Data availability

Data will be made available on request.

## Acknowledgements

We acknowledge supports from the National Science Foundation of China (42101082, 41888101, and 42130507), the Natural Science Foundation of Fujian Province (2023J10496), the Swedish Formas project (2017–01408), the Strategic Priority Research Program of the Chinese Academy of Sciences (XDB26020000) and fellowship for Youth Talent Support Program of Fujian Province.

## Supplementary materials

Supplementary material associated with this article can be found, in the online version, at doi:10.1016/j.agrformet.2024.109974.

## References

- Allen, C.D., Macalady, A.K., Chenchouni, H., Bachelet, D., McDowell, N., Vennetier, M., et al., 2010. A global overview of drought and heat-induced tree mortality reveals emerging climate change risks for forests. *For. Ecol. Manage.* 259, 660–684.
- Adams, H.D., Guardiola-Claramonte, M., Barron-Gafford, G.A., 2009. Temperature sensitivity of drought-induced tree mortality portends increased regional die-off under global-change-type drought. *Proc. Natl. Acad. Sci. U.S.A.* 106, 7063–7066.
- Amoroso, M.M., Daniels, L.D., Villalba, R., Cherubini, P., Paruelo, José., 2015. Does drought incite tree decline and death in austrocedrus chilensis forests? *J. Vegetation Sci.* 26, 1171–1183.
- Ashraf, M., Harris, P.J.C., 2013. Photosynthesis under stressful environments: an overview. *Photosynthetica* 51, 163–190.
- Bai, M., Yao, Q., Camarero, J.J., Hu, H., Dong, Z., Li, Y., Zhou, F., Chen, X., Guo, G., Cao, X., Fang, K., 2021. El nio-southern oscillation modulates insect outbreaks in humid subtropical China: evidences from tree rings and carbon isotopes. *Dendrochronologia (Verona)* 66, 125815.
- Bigler, C., Veblen, T.T., 2009. Increased early growth rates decrease longevity of conifers in subalpine forests. *Oikos* 118, 1130–1138.
- Buckley, B.M., Duangsataporn, K., Palakit, K., Butler, S., Syhpanya, V., Xaybouangeun, N., 2007. Analyses of growth rings of *Pinus merkusii* from Lao PDR. *For. Ecol. Manage.* 253, 120–127.
- Camarero, J.J., Gazol, A., Sangüesa-Barreda, G., Oliva, J., Vicente-Serrano, S.M., 2015. To die or not to die: early warnings of tree dieback in response to a severe drought. *Journal of Ecology* 103, 44–57.
- Chen, D., Fang, K., Li, Y., Dong, Z., Zhang, Y., Zhou, F., 2016. Response of *Pinus taiwanensis* growth to climate changes at its southern limit of Daiyun Mountain, mainland China Fujian Province. *Science China-Earth Sci.* 59, 328–336.
- Choat, B., Jansen, S., Brodribb, T.J., Cochard, H., Delzon, S., Bhaskar, R., Bucci, S.J., Feild, T.S., Gleason, S.M., Hacke, U.G., Jacobsen, A.L., Lens, F., Maherali, H., J Martínez-Vilalta, J., Mayr, S., Mencuccini, M., Mitchell, P.J., Nardini, A., Pittermann, J., Pratt, R.B., Sperry, J.S., Westoby, M., Wright, I.J., Zanne, A.E., 2012. Global convergence in the vulnerability of forests to drought. *Nature* 491, 752–755.
- Colangelo, M., Camarero, J.J., Borghetti, M., Gazol, A., Gentilesca, T., Ripullone, F., 2017. Size matters a lot: drought-affected Italian oaks are smaller and show lower growth prior to tree death. *Front. Plant Sci.* 8.
- Cook, E.R., 1985. A Time Series Analysis Approach to Tree-Ring Standardization. University of Arizona, Tucson, p. 171.
- Coplen, T.B., 1995. Discontinuance of SMOW and PDB. *Nature* 375, 285–285.
- Cuny, H.E., Rathgeber, C.B.K., Frank, D., Font, P., Fournier, M., 2014. Kinetics of tracheid development explain conifer tree-ring structure. *New Phytologist* 203, 1231–1241.
- Evans, M.N., Reichert, B.K., Kaplan, A., Anchukaitis, K.J., Vaganov, E.A., Hughes, M.K., et al., 2006. A forward modeling approach to paleoclimatic interpretation of tree-ring data. *J. Geophys. Res.* 111, G03008.
- Fang, K., Frank, D., Zhao, Y., Zhou, F., Seppä, H., 2015. Moisture stress of a hydrological year on tree growth in the Tibetan Plateau and surroundings. *Environ. Res. Letters* 10, 034010.
- Fensham, R.J., Fairfax, R.J., Ward, D.P., 2009. Drought-induced tree death in savanna. *Glob. Chang. Biol.* 15, 380–387.
- Fonti, P., Babushkina, E.A., 2016. Tracheid anatomical responses to climate in a forest-steppe in Southern Siberia. *Dendrochronologia (Verona)* 39, 32–41.
- Fonti, P., von Arx, G., García-González, I., Eilmann, B., Sass-Klaassen, U., Gärtner, H., Eckstein, D., 2010. Studying global change through investigation of the plastic responses of xylem anatomy in tree rings. *New Phytologist* 185, 42–53.
- Gates, D.M., 1980. *Biophysical Ecology* Springer-Verlag, p. 611. New York.
- Green, J.W., 1963. Methods in carbohydrate chemistry. In: Whistler, R.L. (Ed.), *Wood Cellulose*. Proc 3th Academic Press, New York, pp. 9–21.
- Grissom, R.J., Kim, J.J., 2012. *Effect Sizes For research: Univariate and Multivariate Applications*, 2nd edn. Routledge, New York.
- He, M., Shishov, V., Kaparova, N., Yang, B., Bräuning, A., Grieflinger, J., 2016. Process-based modeling of tree-ring formation and its relationships with climate on the Tibetan Plateau. *Dendrochronologia (Verona)* 42, 31–41.
- Heres, A., Camarero, J.J., López, B.C., Martínez-Vilalta, J., 2014. Declining hydraulic performances and low carbon investments in tree rings predate Scots pine drought-induced mortality. *Trees* 28, 1737–1750.
- Holmes, R., 1983. Computer-assisted quality control in tree-ring dating and measurement. *Tree-ring. Bulletin* 43, 69–78.
- Jing, M., Zhu, L., Liu, S., Cao, Y., Zhu, Y., Yan, W., 2022. Warming-induced drought leads to tree growth decline in subtropics: evidence from tree rings in central China. *Front. Plant Sci.* 13, 964400.
- Kunert, N., Hajek, P., Hietz, P., Morris, H., Rosner, S., Tholen, D., 2021. Summer temperatures reach the thermal tolerance threshold of photosynthetic decline in temperate conifers. *Plant Biol.* 24, 1254–1261.
- Leavitt, S.W., 2008. Tree-ring isotopic pooling without regard to mass: no difference from averaging  $\delta^{13}\text{C}$  values of each tree. *Chem. Geol.* 252, 52–55.
- Leavitt, S.W., Long, A., 1984. Sampling strategy for stable carbon isotope analysis of tree rings in pine. *Nature* 311, 145–147.
- Li, Y., Fang, K., Cao, C., Li, D., Gan, Z., 2016. A tree-ring chronology spanning 210 years in the coastal area of southeastern China, and its relationship with climate change. *Clim. Res.* 67, 209–220.
- Liu, J., Su, S., He, Z., Jiang, N., Gu, X., Xu, D., et al., 2020. Relationship between *Pinus taiwanensis* seedling regeneration and the spatial heterogeneity of soil nitrogen in Daiyun Mountain, southeast China. *Ecol. Indic.* 115, 106398.
- Liu, H., Williams, A.P., Allen, C.D., Guo, D.L., Wu, X.C., Anenkhonov, O.A., et al., 2013. Rapid warming accelerates tree growth decline in semi-arid forests of inner Asia. *Glob. Chang. Biol.* 19, 2500–2510.
- Loader, N.J., Robertson, I., Barker, A.C., Switsur, V.R., Waterhouse, J.S., 1997. An improved technique for the batch processing of small wholewood samples to  $\alpha$ -cellulose. *Chem. Geol.* 136, 313–317.
- Lovejoy, S., Schertzer, D., 2006. Multifractals, cloud radiances and rain. *J. Hydrol. (Amst)* 322, 59–88.
- Lutz, J.A., Halpern, C.B., 2006. Tree mortality during early forest development: a long-term study of rates, causes, and consequences. *Ecol. Monogr.* 76, 257–275.
- Marchin, R.M., Backes, D., Ossola, A., Leishman, M.R., Tjoelker, M.G., Ellsworth, D.S., 2021. Extreme heat increases stomatal conductance and drought-induced mortality risk in vulnerable plant species. *Glob. Chang. Biol.* 28, 1133–1146.
- McCarroll, D., Loader, N.J., 2004. Stable isotopes in tree rings. *Quat. Sci. Rev.* 23, 771–801.
- McDowell, N.G., Beerling, D.J., Breshears, D.D., Fisher, R.A., Raffa, K.F., Stitt, M., 2011. The interdependence of mechanisms underlying climate-driven vegetation mortality. *Trends Ecol. Evol. (Amst.)* 26, 523–532.
- Millar, C.I., Stephenson, N.L., 2015. Temperate forest health in an era of emerging megadisturbance. *Science (1979)* 349, 823–826.
- Minorsky, P.V., 2003. The decline of sugar maples (*Acer saccharum*). *Plant Physiol.* 133, 441–442.
- Mosmann, V., Castro, A., Fraile, R., Dessens, J., Sánchez, J.L., 2004. Detection of statistically significant trend in the summer precipitation of mainland Spain. *Atmos. Res.* 70, 43–53.
- Pacheco, A., Camarero, J.J., Ribas, M., Gazol, A., Gutiérrez, E., Carrer, M., 2018. Disentangling the climate-driven bimodal growth pattern in coastal and continental Mediterranean pine stands. *Sci. Total Environ.* 615, 1518–1526.
- Pellizzari, E., Camarero, J.J., Gazol, A., Sangüesa-Barreda, G., Carrer, M., 2016. Wood anatomy and carbon-isotope discrimination support long-term hydraulic deterioration as a major cause of drought-induced dieback. *Glob. Chang. Biol.* 22 (6), 2125–2137.
- Peñuelas, J., Hunt, J.M., Ogaya, R., Jump, A.S., 2008. Twentieth century changes of tree-ring  $\delta^{13}\text{C}$  at the southern range-edge of *Fagus sylvatica*: increasing water-use efficiency does not avoid the growth decline induced by warming at low altitudes. *Glob. Chang. Biol.* 14, 1076–1088.
- Petrucchi, L., Nardini, A., von Arx, G., Saurer, M., Cherubini, P., 2017. Isotope signals and anatomical features in tree rings suggest a role for hydraulic strategies in diffuse drought-induced die-back of *Pinus nigra*. *Tree Physiol.* 37, 523–535.
- Puchi, P.F., Camarero, J.J., Battipaglia, G., Carrer, M., 2021. Retrospective analysis of wood anatomical traits and tree-ring isotopes suggests site-specific mechanisms triggering *Araucaria araucana* drought-induced dieback. *Glob. Chang. Biol.* 27, 6394–6408.
- Sánchez-Salguero, R., Camarero, J.J., Carrer, M., Gutiérrez, E., Alla, A.Q., Andreu-Hayles, L., et al., 2017a. Climate extremes and predicted warming threaten Mediterranean Holocene fir forests refugia. *Proc. Natl. Acad. Sci. U.S.A.* 114, 201708109.
- Sánchez-Salguero, R., Camarero, J.J., Gutiérrez, E., Rouco, F.G., Gazol, A., Sangüesa-Barreda, G., et al., 2017b. Assessing forest vulnerability to climate warming using a process-based model of tree growth: bad prospects for rear-edges. *Glob. Chang. Biol.* 23, 2705–2719.
- Schweingruber, F.H., 1990. *Anatomy of European woods*. Paul Haupt.
- Shi, J., Liu, Y., Vaganov, E.A., Li, J., Cai, Q., 2008. Statistical and process-based modeling analyses of tree growth response to climate in semi-arid area of North Central China: a case study of *Pinus tabulaeformis*. *J. Geophys. Res.* 113, G01026.
- Soliz-Gamboa, C.C., Ceccantini, G., Angyalossy, V., Van Der Borg, K., Zuidema, P.A., 2011. Evaluating the annual nature of juvenile rings in Bolivian tropical rainforest trees. *Trees* 25, 17–27.

- Song, Y., Chen, Q., Dong, C., Shao, X., Zhang, D., 2014. Effects of high temperature on photosynthesis and related gene expression in poplar. *BMC Plant Biol.* 14, 111.
- Sneyers, R., 1991. Technical note. World Meteorological Organization.
- Timofeeva, G., Treydte, K., Bugmann, H., Rigling, A., Schaub, M., Siegwolf, R., Saurer, M., 2017. Long-term effects of drought on tree-ring growth and carbon isotope variability in Scots pine in a dry environment. *Tree Physiol.* 37, 1028–1041.
- Vaganov, E.A., Hughes, M.K., Shashkin, A.V., 2006. Growth dynamics of conifer tree rings: images of past and future environments. *Ecol. Studies* 183.
- van Mantgem, P.J., Stephenson, N.L., Byrne, J.C., Daniels, L.D., Franklin, J.F., Fule, P.Z., et al., 2009. Widespread increase of tree mortality rates in the western United States. *Science* (1979) 323, 521–524.
- Wigley, T.M.L., Briffa, K.R., Jones, P.D., 1984. On the average value of correlated time series, with applications in dendroclimatology and hydrometeorology. *J. Climatol. Appl. Meteorol.* 23, 201–213.
- Wong, C.M., Daniels, L.D., 2017. Novel forest decline triggered by multiple interactions among climate, an introduced pathogen and bark beetles. *Glob. Chang. Biol.* 23, 1926–1941.
- Zhang, R., Hu, Z., Cherubini, P., Cooper, D.J., Zhu, L., Lei, P., 2023. Tree-ring data reveal trees are suffering from severe drought stress in the humid subtropical forest. *For. Ecol. Manage.* 546, 121330.
- Zheng, Z., 2023. PhD thesis. Fujian Normal University.
- Zhou, F., Fang, K., Zhang, F., Dong, Z., 2019. Hydroclimate Change encoded in tree rings of Fengshui woods in Southeastern China and its teleconnection with El Niño–Southern Oscillation. *Water Resource Res.* 56, e2018WR024612.
- Zhu, D., 2013. Master's Dissertation. Fujian Agriculture and Forestry University.